Colloidal Swarms Can Settle Faster than Isolated Particles: Enhanced Sedimentation near Phase Separation

Enrico Lattuada, Stefano Buzzaccaro, and Roberto Piazza*
Department of Chemistry, Material Science, and Chemical Engineering "G. Natta", Politecnico di Milano, Piazza Leonardo da Vinci 32, 20133 Milano, Italy

(Received 22 October 2015; revised manuscript received 18 December 2015; published 21 January 2016)

By experimenting on model colloids where depletion forces can be carefully tuned and quantified, we show that attractive interactions consistently "promote" particle settling, so much that the sedimentation velocity of a moderately concentrated dispersion can even exceed its single-particle value. At larger particle volume fraction ϕ, however, hydrodynamic hindrance eventually takes over. Hence, $v(\phi)$ actually displays a nonmonotonic trend that may threaten the stability of the settling front to thermal perturbations. Finally, by discussing a representative case, we show that these results are relevant to the investigation of protein association effects by ultracentrifugation.

DOI: 10.1103/PhysRevLett.116.038301

Natural settling of particulate plays a crucial role in geology and environmental science, while forced sedimentation (centrifugation) has countless applications in the primary and manufacturing industry and as a preparative and analytic method in biology and medicine. Besides its practical usefulness, colloid sedimentation has been highly influential in the development of statistical physics too, thanks to the celebrated experiments by Perrin [1] that provided a concrete demonstration of molecular reality and gave full support to Einstein's theory of Brownian motion. Several recent investigations made in the footsteps of Perrin's work have shown that equilibrium settling profiles yield extensive and sometimes surprising information on the equation of state and phase behavior of model colloidal suspensions of hard, "sticky," charged, magnetic, and even active Brownian particles [2].

Yet, while the investigation of equilibrium sedimentation has reached a rather mature stage, full understanding of the settling kinetics is still precluded by substantial experimental and theoretical challenges, because of the overwhelming intricacies brought in by the presence of solvent-mediated hydrodynamic interactions (HIs) between the particles. In fact, the long-ranged, many-body nature of HI leads to a diverging expression for the settling velocity of a colloidal suspension, however dilute, unless the renormalizing effect of solvent counterflow in a finite container is carefully taken into account. This crucial observation is at the heart of the seminal result obtained by Batchelor [3] in 1972, who showed that, at first order in particle volume fraction ϕ, the settling velocity of a suspension of hard spheres (HS) is given by $v_{\mathrm{HS}}(\phi) = v_s(1 - 6.55\phi)$, where $v_s = 2\Delta\rho g R^2/9\eta$ is the Stokes settling speed of a single sphere of radius R in terms of the density difference $\Delta\rho$ with the solvent and of the solvent viscosity η. Batchelor's expression [4] embodies the concept of *hindered settling*, namely, that for HS, hydrodynamic interactions slow down settling, yielding a sedimentation velocity which decreases with particle concentration. One of the most important consequences of hindered settling is that the equation governing sedimentation assumes a Burgers-like structure [5,6]: this means that, after a transient period, the sedimentation front takes on a time-invariant shape dictated by the competition between the ϕ-dependent settling velocity, which sharpens the interface with the supernatant, and Brownian diffusion, which conversely spreads the front.

However, collective effects do not *necessarily* result in hindered settling, because attractive interparticle forces may effectively counteract hydrodynamic interactions. Ten years later, Batchelor extended his approach to generic interparticle interactions beyond the HS model, finding, still at first order in ϕ [7]

$$\frac{v(\phi)}{v_s} = 1 - [6.55 - 3.52(1 - B_2^*)]\phi, \tag{1}$$

where B_2^* is the ratio between the second osmotic virial coefficient B_2 of the suspension and the same quantity for HS ($B_2^{\mathrm{HS}} = 4$ for a virial expansion in ϕ). According to Eq. (1), the settling velocity becomes even *larger* than the Stokes velocity v_s when $B_2^* \lesssim -0.86$ ($B_2 \lesssim -3.44$). This means that attractive interactions, if sufficiently strong, may *promote* rather than hinder sedimentation so that a colloidal swarm may even settle faster than a single isolated particle. A consistent reduction of the dependence on ϕ of the settling velocity was first detected by Jansen *et al.* [8] for suspensions of silica particles in toluene, where attractive interactions can be switched on by lowering the temperature, although just a semiquantitative explanation of the effect could be given due to the lack of a precise form of the interaction potential. To our knowledge, however, no direct and quantitative confirmation of the most striking prediction of Eq. (1), that of "promoted" sedimentation, has so far been given for simple model colloids. Recently, the survey

of attractive particle sedimentation has been extended to higher volume fractions by Moncho-Jordá *et al.* [9], who exploited numerical simulations to show that the settling velocity becomes, in fact, *nonmonotonic* in ϕ, because at sufficiently large ϕ the hindering effect of HI becomes dominant even for strongly attractive colloids.

Here, by using a model colloidal system where the interparticle interaction potential can be carefully tuned, we plan to show that promoted settling can be clearly unraveled and that the predictions made in Ref. [9] can be confirmed and quantitatively tested. Besides, we highlight a subtle consequence of these results, namely, that self-sharpening of the settling front to a time-invariant "shock-wave" profile no more holds and that promoted settling rather leads to a "stretching" of the profile, which may eventually lead to instability and stratification. Finally, using a specific example, we discuss our results in the related context of ultracentrifugation studies of proteins undergoing weak association effects.

The system we used consists of monodisperse spherical particles with a radius $R = 90 \pm 3$ nm made of MFA, a polytetrafluoroethylene copolymer [10], suspended in solutions of Triton X100, a nonionic surfactant that forms globular micelles with a radius $a \simeq 3.5$ nm, acting as a depletant for the MFA particles. Former measurements of equilibrium sedimentation profiles provided a full characterization of this system in terms of equation of state and phase diagram, allowing a detailed quantitative mapping of the suspension onto a model system of adhesive hard spheres (AHS, [11,12]). The interaction potential $U(r)$ between AHS of diameter σ is described by the Boltzmann factor (with $\beta = k_B T$)

$$e^{-\beta U(r)} = \Theta(r-\sigma) + \frac{\sigma}{12\tau}\delta(r-\sigma). \tag{2}$$

The Heaviside function Θ accounts for the hard-core repulsion, while the second term represents an attraction at contact with a strength inversely proportional to the "stickiness" parameter τ [13]. Additional information on the phase behavior of the AHS model is given in Refs. [14–17] and in the Supplemental Material [18]. For what follows, it is useful to note that this system displays, for values of $\tau < \tau_c \simeq 0.113$, a wide metastable gas-liquid coexistence region [13]. Consistent effects on $v(\phi)$ may then be expected in the one-phase region close to the gas-liquid binodal line, where attractive forces are very strong.

Measurements of the settling velocity were performed using an analytical centrifuge (LUMiSizer, Lum GmbH), which allows us to monitor simultaneously the settling kinetics of up to 12 samples by measuring their optical extinction profile with a linear detector array with an accurate temperature control in the range $4\ ^\circ\text{C} \leq T \leq 40\ ^\circ\text{C}$. For a concentrated dispersion, this usually yields just a semiquantitative concentration profile, because the sample transmittance depends not only on concentration but also on the suspension structure. The major advantage of using MFA colloids is that the partial crystallinity of these particles originates an incoherent scattering contribution which does not depend on particle interactions [10]. Therefore, if the coherent scattering contribution is suppressed by adding a moderate amount of urea or glycerol, so to match the particle average refractive index ($n_p \simeq 1.352$) with that of the solvent, the sample absorption (more properly, natural extinction) A is strictly proportional to the local particle volume fraction. Like in Ref. [12], all measurements were performed in the presence of a substantial amount of added salt (NaCl 250 mM) to screen electrostatic interactions between the particles, which are stabilized by a layer of the same surfactant acting as depletant (for details, see the Supplemental Material [18]).

We first discuss the results for the sedimentation velocity obtained at fixed particle volume fraction $\phi = 0.04$ as a function of the strength of the depletion interactions, varied by increasing the amount of added surfactant. Since the second osmotic virial coefficient of AHS is given by $B_2^* = 1 - (4\tau)^{-1}$, Eq. (1) predicts, for $\phi = \phi_0 = 0.04$,

$$\frac{v_{\text{AHS}}(\tau)}{v_s} = 0.738 + 0.0352\tau^{-1}. \tag{3}$$

Quantitative assessment of the strength of attractive interactions requires, however, a careful mapping of the stickiness parameter on depletant concentration c. This can be made by exploiting the principle of extended corresponding states [19], which allows us to map an AHS system onto the Asakura-Oosawa (AO) model for depletion interactions by equating the values of B_2, a strategy which has already been successfully adopted in a previous study [20]. The $\tau(c)$ mapping obtained by this method, which is further discussed in the Supplemental Material [18], is shown in the inset of Fig. 1. The dependence of the settling velocity on τ scaled to the single-particle Stokes velocity is displayed in the main part of Fig. 1. The data show that, for $\tau^{-1} \lesssim 1.5$, $v(\tau)$ grows indeed linearly with τ^{-1}, with a slope that fully agrees with Eq. (3) but with an experimental intercept which is about 5% larger than predicted. This is arguably due to the limited accuracy of Batchelor's first-order approximation for HS, even for volume fractions as low as 4%. In fact, the more elaborated expression obtained by Hayakawa and Ichiki [21], which reasonably accounts for $v_{\text{HS}}(\phi)$ up to the limit of the fluid phase ($\phi \simeq 0.50$), yields a value of 0.78 that fully agrees with the experiment. For $\tau^{-1} \gtrsim 1.5$, the approximation at order ϕ in Eq. (3) seems, however, to overestimate the effect of attractive interactions.

Observing a sedimentation velocity larger than the *single*-particle value v_s requires us, however, to increase τ^{-1} further, still keeping it below the phase-separation limit. Yet, because of the huge, quasiexponential dependence of the stickiness parameter on c (see the inset in Fig. 1, where τ^{-1} more than doubles by increasing c by less than 1%),

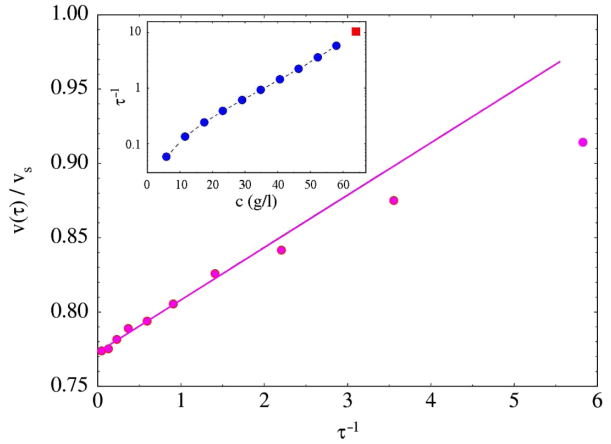

FIG. 1. Inset: Values of τ^{-1} as a function of the surfactant concentration c obtained by virial coefficient matching as discussed in the text and in the Supplemental Material [18]. The square indicates the value $\tau_{PS}^{-1} \simeq 10.5$ where phase separation is experimentally observed at $\phi = 0.04$, which is slightly higher than the critical value $\tau_c^{-1} \simeq 8.8$ (at $\phi_c \simeq 0.26$) for AHS. Main figure: Settling velocity $v(\tau)$ for MFA suspensions at fixed particle volume fraction $\phi = 0.04$ and temperature $T = 25$ °C, as a function of τ^{-1}. The straight line is drawn from the measured value for hard spheres $v_{HS}/v_s \simeq 0.77$, with the slope given by Eq. (3).

accurate dosing of the depletant in this narrow range is experimentally prohibitive. Much finer tuning can be obtained by exploiting the temperature dependence of depletion interactions in the system we investigate, which grow with T because of the increasing correlation between the depletant micelles [22]. As a rough figure, the same strengthening of attractive forces due to an increase of surfactant concentration by 0.1% is obtained by raising T by 0.5 °C, which is much easier to control. Exploiting virial coefficient matching is, in this case, less straightforward, since, approaching depletant phase separation, the interaction potential progressively deviates from the simple AO form, becoming longer ranged [22]. Tentatively, however, the increase of depletion forces can be accounted for by a simple rescaling $c \to c^*(T)$ of the depletant concentration. As detailed in the Supplemental Material [18], such a rescaling can be done by measuring, at fixed ϕ, the T dependence of the depletant concentration $c_{PS}(T)$ where phase separation is first observed. For $\phi = 0.04$, c_{PS} is found to decrease with T as $c_{PS}(T) \simeq c_{PS}(25)(1.47 - 0.019T)$, where $c_{PS}(25)$ is the depletant concentration required for phase separation at $T = 25$ °C. Hence, the approach we followed simply consists in assuming $c^*(T) = [c_{PS}(25)/c_{PS}(T)]c$ and using virial coefficient mapping on the AO potential to obtain τ. The effectiveness of this strategy was checked by comparing the entire phase-separation line $\tau(\phi)$ obtained by this method with numerical simulation results [13].

We have then measured the volume fraction dependence of $v(\phi)$ up to $\phi = 0.2$ at fixed depletant concentration $c = 56$ g/l. Figure 2 shows that the behavior of $v(\phi)$ drastically changes by increasing the temperature from $T = 25$ °C corresponding to $\tau \simeq 0.2$, up to $T = 30$ °C ($\tau \simeq 0.12$), which is the highest temperature we managed to work at without incurring phase separation over the whole ϕ range [23]. At $T = 25$ °C, the settling velocity decreases monotonically with ϕ, although with a trend which drastically differs from what was predicted and observed for HS [21], also shown in the figure for comparison. At $T = 30$ °C, $v(\phi)$ displays a nonmonotonic trend characterized by a maximum at $\phi \simeq 0.06 - 0.08$ and is definitely *larger* than v_s up to $\phi \simeq 0.13$. Qualitatively, this behavior can be understood by considering that attractive interactions promote settling at low ϕ, while for dense systems, where the excluded volume contribution becomes dominant, the slowing-down effect of HI eventually takes over. As we mentioned, a very similar trend has been found by mesoscopic simulations based on stochastic rotation dynamics (SRD) [9], which already proved successful in reproducing hydrodynamic fluctuations in sedimentation [24]. Although the values of B_2^* used in Ref. [9] do not exactly coincide with those we investigated ($B_2^* = -0.27$ at $T = 25$ °C, $B_2^* = -1.08$ at 30 °C), their results can easily be interpolated to obtain the curves shown by open symbols in Fig. 2, which

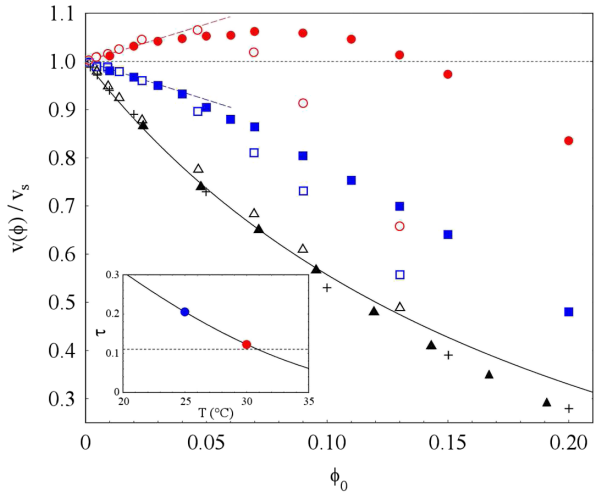

FIG. 2. Inset: Full dependence of τ on T obtained for $c = 56$ g/l using the mapping strategy discussed in the text and detailed in the Supplemental Material [18]. Main figure: Normalized settling velocity as a function of the initial particle volume fraction ϕ obtained for $\tau = 0.21$ ($T = 25$ °C, filled square) and $\tau = 0.12$ ($T = 30$ °C, filled circle) at fixed surfactant concentration $c = 56$ g/l. The corresponding open symbols are results from numerical simulations obtained by interpolating the set of results presented in Ref. [9]. Dotted lines show the low-ϕ linear behavior predicted by Batchelor's expression (1). The figure also compares the data obtained for MFA suspensions in the absence of added surfactant (filled triangle) with the SRD results for HS (open triangle), together with analytical (full line [21]) and numerical (+ [25]) results for $v_{HS}(\phi)$.

qualitatively show the same distinct trends observed in the experiments. Quantitatively, however, predictions for $\tau = 0.12$ display a much larger curvature, yielding a more restricted range where promoted settling should be observed. It should, however, be noticed that to reproduce the correct hydrodynamics of hard spheres, SRD simulations require the authors in Ref. [9] to use an effective particle size which is about 20% smaller than the HS radius, yielding, of course, an effective ϕ about a factor of 2 smaller. Whether this prescription is valid in the presence of strong interactions too is an open question.

Promoted settling may, however, have a drastic and so far unnoticed consequence on the settling kinetics. Self-sharpening of the interface into a time-invariant, shock-wave profile *requires* hindered settling, namely, that $v(\phi)$ decreases with ϕ. In fact, self-sharpening can be qualitatively understood by observing that the dilute particle "fan" left beyond by diffusion settles faster, rapidly catching the settling front. Promoted settling may conversely be expected to induce a progressive expansion of the interface separating the settling suspension from the supernatant solvent so that the profile would stretch in time, never reaching a stationary shape. This prediction is confirmed by contrasting the kinetic settling profiles shown in the two panels of Fig. 3. Whereas in the absence of added surfactant (upper panel) the interface rapidly takes on an almost invariant shape [26], the profile for a depleted colloid progressively stretches in time. It is useful to point out that, in the presence of even minimal lateral temperature gradients, a stretching interface may become unstable, leading to stratification and formation of a banded profile. Although known for almost a century [27], this curious effect has usually been observed for extremely dilute

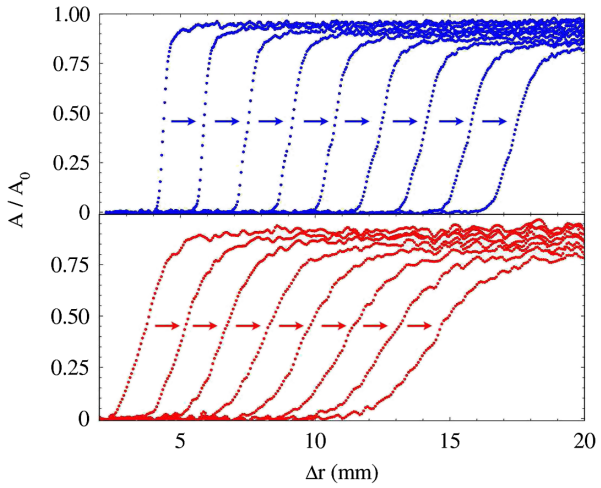

FIG. 3. Comparison between the settling profiles obtained at $T = 30$ °C for MFA suspensions at $\phi = 0.04$ without added surfactant (top) and in the presence of a depletant concentration $c = 56$ g/l, corresponding to $\tau \simeq 0.12$ (bottom). In both panels, Δr is the displacement from the position of the top of the initially homogeneous suspension.

dispersions, where substantial spreading of the interface takes place *before* it reaches a time-invariant shape [28,29]. Our evidence suggests that stratified settling may also occur in rather concentrated suspensions of strongly attractive monodisperse particles.

The evidence we discussed, although obtained for a simple model system, may also be relevant for the investigation of macromolecular association processes, a field of considerable biological importance. In fact, settling velocities larger than v_s have long been observed in ultracentrifuge (UC) studies of associating proteins (for a review, see Ref. [30]). Recent instrumental advances have, indeed, significantly improved the capability and sensitivity of analytical UC, generating a consistent "revival" of this old but extremely powerful method to detect protein association [31]. In protein biochemistry, these processes are usually modeled as a dynamical equilibrium between monomers and oligomeric species, whose aggregation number and structure are dictated by the specific stereochemistry of the involved proteins. In fact, for rapidly reversible aggregation (binding energy not too large compared to k_BT) these "chemical reaction" models do predict a settling velocity that increases with protein concentration. Chemical reaction models, however, fully neglect hydrodynamic interactions, which are the simplest, if not the only responsible for the *decrease* of $v(\phi)$ at sufficiently high concentration. That nonspecific, "physical" interactions can also affect UC measurements was pointed out long ago by Nichol and Ogston [32], who, in their general study of moving interfaces, also extensively discuss interface spreading when $dv(\phi)/d\phi > 0$. In fact, the nontrivial "reaction boundaries" arising in the centrifugation of macromolecular aggregates whose lifetime is short compared to the characteristic settling time are still extensively investigated [33,34]. Here too, HI should be carefully taken into account.

An emblematic example to which all the former considerations apply is that of β-lactoglobulin A (BLGA) [35], a globular protein which, in a narrow pH and temperature range, undergoes a weak but extensive association process. In these conditions, UC measurements evidence both promoted settling and a nonmonotonic behavior of $v(\phi)$ [36]. Later, light scattering (LS) results, however, showed that BLGA aggregates have an extremely short lifetime so that they should be regarded as transient clusters [37,38]. A combination of static and dynamic LS data allowed the authors of Ref. [38], moreover, to determine the full concentration dependence, as a function of T, of the so-called "hydrodynamic factor" $H(\phi)$, which directly yields the sedimentation velocity as $v(\phi) = v_s H(\phi)$. Notably, $H(\phi)$ turns out to be nonmonotonic in ϕ, with a maximum around the concentration value where the highest settling speed is observed. An explicit comparison of LS and UC data showing a remarkable quantitative agreement for the magnitude and concentration dependence of $v(\phi)/v_s$ is

presented in the Supplemental Material [18]. By combining scattering and ultracentrifugation measurements, several features of protein association effects can then be figured out using well-established concepts in colloid physics, without necessarily resorting to a specific oligomerization model.

We thank A. Vrij and A. P. Philipse for useful discussions. This work has been supported by PRIN 2012 funding from the Italian Ministry of Education, University and Research (MIUR).

*roberto.piazza@polimi.it

[1] J. Perrin, Ann. Chim. Phys. **18**, 5 (1908).
[2] R. Piazza, Rep. Prog. Phys. **77**, 056602 (2014).
[3] G. K. Batchelor, J. Fluid Mech. **52**, 245 (1972).
[4] It is worth noticing that Batchelor's formula is valid only provided that the Péclet number $\mathrm{Pe} = Rv_s/D$, where D is the Brownian diffusion coefficient, is small [2]. All measurements reported in this Letter have been performed at $\mathrm{Pe} \ll 1$.
[5] S. E. Esipov, Phys. Rev. E **52**, 3711 (1995).
[6] S. Buzzaccaro, A. Tripodi, R. Rusconi, D. Vigolo, and R. Piazza, J. Phys. Condens. Matter **20**, 494219 (2008).
[7] G. K. Batchelor, J. Fluid Mech. **119**, 379 (1982).
[8] J. W. Jansen, C. G. D. Kruif, and A. Vrij, J. Colloid Interface Sci. **114**, 501 (1986).
[9] A. Moncho–Jordá, A. A. Louis, and J. T. Padding, Phys. Rev. Lett. **104**, 068301 (2010).
[10] V. Degiorgio, R. Piazza, T. Bellini, and M. Visca, Adv. Colloid Interface Sci. **48**, 61 (1994).
[11] R. Baxter, J. Chem. Phys. **49**, 2770 (1968).
[12] S. Buzzaccaro, R. Rusconi, and R. Piazza, Phys. Rev. Lett. **99**, 098301 (2007).
[13] M. A. Miller and D. Frenkel, J. Chem. Phys. **121**, 535 (2004).
[14] G. Stell, J. Stat. Phys. **63**, 1203 (1991).
[15] D. Frenkel, Physica (Amsterdam) **263A**, 26 (1999).
[16] P. R. ten Wolte and D. Frenkel, Science **277**, 1975 (1997).
[17] R. P. Sear, J. Chem. Phys. **111**, 2001 (1999).
[18] See Supplemental Material at http://link.aps.org/supplemental/10.1103/PhysRevLett.116.038301 for information about the phase behavior of the investigated system and on the methods used to obtain the τ parameter.
[19] M. G. Noro and D. Frenkel, J. Chem. Phys. **113**, 2941 (2000).
[20] S. Buzzaccaro, R. Piazza, J. Colombo, and A. Parola, J. Chem. Phys. **132**, 124902 (2010).
[21] H. Hayakawa and K. Ichiki, Phys. Rev. E **51**, R3815 (1995).
[22] S. Buzzaccaro, J. Colombo, A. Parola, and R. Piazza, Phys. Rev. Lett. **105**, 198301 (2010).
[23] Phase separation can easily be detected by the sudden increase of the sample turbidity associated to spinodal decomposition.
[24] J. T. Padding and A. A. Louis, Phys. Rev. Lett. **93**, 220601 (2004).
[25] A. J. C. Ladd, J. Chem. Phys. **93**, 3484 (1990).
[26] Time invariance of the profile holds rigorously true only in natural gravity. In a centrifuge, where the local acceleration may spatially vary by 20%–30% within the measurement region, the profile slightly "stretches" in time. For the same reason, the concentration of the settling "column," which in natural gravity is constant, slightly decreases in time, as evident in Fig. 3.
[27] C. E. Mendenhall and M. Mason, Proc. Natl. Acad. Sci. U.S.A. **9**, 199 (1923).
[28] D. B. Siano, J. Colloid Interface Sci. **68**, 111 (1979).
[29] A. V. Butenko, P. M. Nanikashvili, D. Zitoun, and E. Sloutskin, Phys. Rev. Lett. **112**, 188301 (2014).
[30] L. M. Gilbert and G. Gilbert, in *Enzyme Structure, Part D*, edited by N. P. Kaplan, N. P. Colowick, C. Hirs, and S. N. Timasheff, Methods in Enzymology Vol. 27 (Academic Press, New York, 1973), pp. 273–296.
[31] J. Liu, J. D. Andya, and S. J. Shire, AAPS J. **8**, E580 (2006).
[32] L. W. Nichol and A. G. Ogston, Proc. R. Soc. B **163**, 343 (1965).
[33] P. Schuck, Biophys. J. **98**, 2005 (2010).
[34] D. Mercadante, L. D. Melton, G. E. Norris, T. S. Loo, M. A. K. Williams, R. C. J. Dobson, and G. B. Jameson, Biophys. J. **103**, 303 (2012).
[35] For the detailed molecular structure of BLGA, see RCSB Protein Data Bank, structure i.d. 1beb, http://www.rcsb.org/pdb/explore/explore.do?structureId=1beb.
[36] R. Townend, R. J. Winterbottom, and S. N. Timasheff, J. Am. Chem. Soc. **82**, 3161 (1960).
[37] R. Piazza and S. Iacopini, Eur. Phys. J. E **7**, 45 (2002).
[38] R. Piazza, S. Iacopini, and M. Galliano, Europhys. Lett. **59**, 149 (2002).

E. Lattuada, S. Buzzaccaro, and R. Piazza

Supplemental Material

These notes provide, after a short introduction to the phase behavior of an AHS system, a concise description of the methods we applied to obtain the values of the AHS stickiness parameter τ. This is the strategy used in the main text to describe the results for the settling velocity obtained by varying either the depletant concentration c at fixed temperature T, or T at fixed c.

1 The Adhesive Hard Spheres model

Consider a system of spherical colloidal particles of diameter σ interacting, in addition to the excluded volume term, via effective attractive forces of characteristic range δ. If δ is sufficiently shorter than σ (typically, when $q = \delta/\sigma \lesssim 1/3$), the critical temperature of the system drops below the triple point temperature, hence the liquid-gas coexistence region becomes metastable with respect to freezing and the system displays a single fluid phase [1]. Within the fluid-solid coexistence region, however, the crystal nucleation rate is consistently quenched with respect to a HS system [2], if exception is made of a narrow region close to the metastable critical point [3]. Hence, the system usually remains in a metastable fluid phase for very long time, which opens up the possibility of investigating colloidal fluids where attractive interactions that are so strong as to lead in principle to crystallization are present. This distinctive behavior is particularly pronounced when $q \ll 1$, which is the case of several systems of noticeable interest, such as globular proteins close to crystallization, and of the depletion system we considered, where (at least far from the depletant critical point) q is about 0.03.

A further interesting feature is that all short-ranged pairwise additive attractive potentials are characterized by the same thermodynamics properties, when compared at the same reduced density and second virial coefficient. Because of this "extended" law of corresponding states, these systems are often suitably described by the simple Adhesive Hard Spheres (or "sticky spheres") model, introduced by Rodney Baxter in 1968 [4], who also provided an analytical solution for its equation of state in the Percus-Yevick approximation. The interaction potential for AHS consists, in addition to the excluded volume term, of a surface adhesion obtained as the limit of a square well potential of vanishing width and increasing depth, carefully taken so to ensure that the 2^{nd} virial coefficient of the pressure expansion in powers of the particle number density ρ

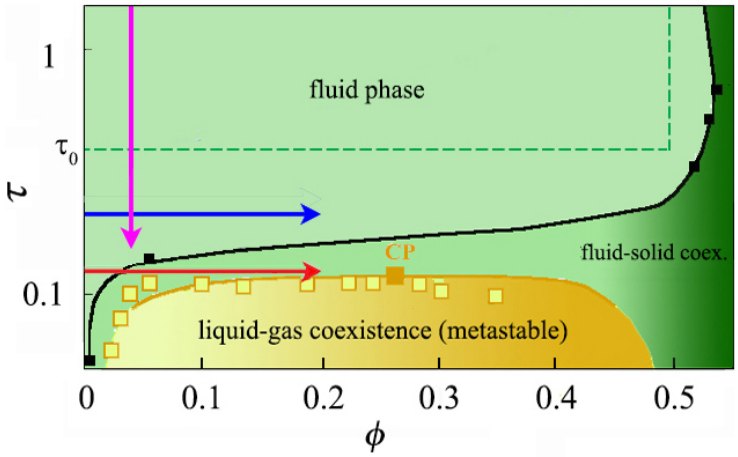

Figure 1: Experimental $\tau - \phi$ phase diagram for the MFA + Triton X100 system in the region of interest for the present work, obtained by equilibrium sedimentation measurements [7]. Full and open squares are the experimental data for the freezing and spinodal line, respectively. The full yellow line shows the numerical result for the coexistence line [5]. Boroken lines border the region of stability of the fluid phase according to the β_0-model for $q = 0.03$. The vertical purple and horizontal blue/red arrows are the paths in the phase diagram investigated in this work (line colors correspond to the data in Fig. 1 and 2 of the text).

(or volume fraction ϕ) remains finite. This limiting behavior, which is conveniently expressed in terms of the Boltzmann factor given by Eq. (2) of the main text, is characterized by a single parameter τ, playing the role of an effective temperature. Numerical simulation of the AHS model yield a critical point at $\tau_c \simeq 0.113$, $\phi_c \simeq 0.266$, and a rather flat coexistence line in which τ varies by no more than 20% in the volume fraction range $0.04 \leq \phi \leq 0.45$ [5].

Actually, for perfectly monodisperse spheres, the AHS is inherently pathological: the virial expansion is not convergent, so that the fluid phase becomes unstable for any finite density. Yet, in the presence of polydispersity of particle size, however small, thermodynamic consistency is recovered [6]. In fact, for short-range attractive systems, polydispersity plays a much stronger role than for HS. While the latter crystallize whenever the relative standard deviation w of the particle size distribution is less than about 10% (which is sensible, since the lattice spacing of the HS crystal is about 1.1σ), for attractive potentials, whose crystal lattice has a spacing of order $(1+\delta/2)\sigma$, polydispersity already becomes relevant when $w \gtrsim \delta$. The AHS cannot of course account for the freezing and melting lines of a real system with a finite attractive range, since its equilibrium state consists of an ordered close-packed crystal at $\phi = \pi/3\sqrt{2} \simeq 0.74$ coexisting with a "void" ($\phi = 0$) fluid phase. The detailed shape of the fluid–solid phase boundaries depend in fact on the specific form of the interaction potential. For

small q, however, a rough approximation of the fluid–solid coexistence can be obtained by the so-called Stell's β_0-model, which basically consists in assuming that the particles behaves like HS for values of $\tau \geq \tau_0 = 1/(12q^{1/2})$, and like AHS for $\tau < \tau_0$ [2]. In fact, when $q \ll 1$, the shape of the numerically evaluated coexisting boundaries for any short-range potentials differ from the straight lines of the β_0-model just because they are a bit "sloped", and because they bend at low ϕ.

As discussed in the main text, equilibrium sedimentation measurements have shown that both the equation of state and the L-G coexistence line of the system investigated in this paper closely conform to what is predicted for a AHS system [7]. A sketch of the region of the experimental phase diagram of interest for this work is presented in Fig. 1. Notably, the experimental values of τ where L-G separation is first observed are in good agreement with the numerical results by Miller and Frenkel [5] for the coexistence line. However, the experimental freezing line obtained from equilibrium sedimentation measurements lies well below the stability limit for the fluid phase obtained from the β_0-model, which is consistent with the comparison with simulation results for a square-well potential presented in Fig. 2 of Ref. [7]. Once again, this arguably means that polydispersity, even if small, substantially increases the stable fluid phase region. The vertical and horizontal arrows show the experimental paths correspondent to the settling measurements discussed in this work, mapped onto the $\tau - \phi$ phase diagram using the methods described in the next two sections. It is worth pointing out that the sample investigated in the measurements corresponding to the red path ($\tau = 0.12$), which mostly lies within L-S coexistence region, do not crystallize over several weeks, which confirms that crystal nucleation is severely quenched, unless very close to the critical point CP.

2 Mapping at fixed temperature ("$c - \tau$ mapping")

As mentioned in the text, in the system we investigate the added surfactant plays both the role of stabilizing and of a depleting agent. In fact, when added to MFA dispersions, the surfactant first adsorbs on the particle surface, progressively forming a monolayer of thickness $\delta \simeq 3$ nm that stabilizes the suspension up to very high ionic strength, until full coverage of the particle surface is reached. Light scattering measurements of the adsorption isotherm show that this takes place for a surfactant concentration $c_{s0} \simeq 0.06\rho_s\phi$, where $\rho = 1.064$ g/cm^3 is the density of Triton X100 and ϕ is the MFA particle volume fraction. As checked by UV spectrophotometry, at $c_s = c_{s0}$ the concentration of free surfactant in solution does not exceed 0.2 g/l. Further surfactant addition results in the formation of globular micelles, acting as a depletant. For any given surfactant concentration $c_s > c_{s0}$, the depletant concentration c used in the text is therefore equal to the concentration $c_s - c_{s0}$ of surfactant in micellar form. The volume fraction ϕ_s of depletant can then be obtained from the values, measured by light

scattering, of the volume V_m and aggregation number N of the micelles [8]

$$\phi_s = \frac{V_m \mathcal{N}_A}{N M_w}(c_s - c_{s0}) \simeq (0.0014 \text{ l/g})\, c, \tag{1}$$

where $M_w = 625$ g/mol is the molecular weight of Triton X100 and $\mathcal{N}_A$ is the Avogadro number.

At fixed temperature, the stickiness parameter τ can be related to ϕ_s by matching the 2$^{\text{nd}}$ osmotic virial coefficient B_2 of an Asakura-Oosawa potential to the AHS model. As detailed in [7], a simple calculation yields:

$$\tau^{-1} = 12q \int_0^1 (1+qx)^2 \left[e^{3\phi_s Z(\phi_s)(1-x)^2/2q} - 1 \right] dx, \tag{2}$$

where q is the ratio between the range of the depletion potential and the particle radius R, x is a dimensionless interparticle separation related to the distance d between two particles by $x = (d-2R)/2Rq$, and corrections for the non-ideality of the depletant solution are embodied in the compressibility factor $Z(\phi_s) = \Pi/nk_BT$. The latter can accurately be obtained by light scattering measurements, yielding at $T = 25°$C:

$$Z(\phi_s) = 1 - 0.12\phi_s + 19\phi_s^2 + O(\phi_s^3) \tag{3}$$

The effective size ratio q, which is the only free parameter in Eq. 2, can finally be obtained by comparing the amount of surfactant required to induce phase separation of a colloidal suspension at a given volume fraction ϕ with the τ value obtained from numerical simulation at the same depletant volume fraction [5]. The experimental value $\phi_s \simeq 0.061$ at $\phi = 0.05$ yields $q \simeq 0.028$, which can reasonably be accounted for by considering that Triton micelles are slightly oblate ellipsoids with major and minor semiaxes equal to $a \simeq 4.8$ nm and $b = 2.4$ nm, and an aggregation number N =145 [8].

3 Temperature mapping at fixed c ("$T - \tau$ mapping")

Like many nonionic surfactants, Triton X100 shows an inverted coexistence gap with water, with a critical concentration $c_c \simeq 20\,$g/l and a lower critical temperature that, in the presence of 250 mM NaCl is $T_c \simeq 63°$ C. Former experiments have shown that, approaching this coexistence gap, the increase of correlation between the surfactant micelles yields a strong increase of the depletion forces, which become temperature-dependent in a wide T-range below the surfactant/water coexistence gap [9]. While mappings of the experimental depletant concentration on an effective stickiness parameter (or reduced virial coefficient B_2^*) have often been used in depletion studies, mapping of $\tau(T)$ for temperature–dependent depletion forces, used for the first time in this work, requires a more detailed description.

By increasing T, the depletant becomes less and less ideal, hence the effective interaction potential between the colloidal particles is no more described by the

simple AO potential, but rather progressively develops a long range tail which is directly related to the increase of the depletant correlation length [9]. In principle, an accurate mapping would therefore require using a T-dependent potential obtained from the model developed in Ref. [9], which should furthermore be validated by measuring for instance the equation of state at different values of T. This could be a very interesting test of the continuity between depletion forces and critical Casimir effects suggested in Ref. [9], but is not required for this work. For our purposes, T is indeed used just as a fine-tuning parameter of the depletion forces, and all measurements are performed more than 30° C below the depletant phase separation region, where "critical" depletion effects become dominant. An experimentally simpler approach consists in assuming that depletion interactions are still approximately described by the AO potential, but with an effectively increased depletant volume fraction, which embodies the effect of the increased correlation length of the depletant[1]. As discussed in the main text, rescaling of the depletant concentration to an effective value $c^*(T)$ can be made by comparing the depletant concentration $c_{ps}(T)$ where phase separation is first observed to the value $c_{ps}(25)$ obtained at 25°C. Fig. 2 shows that $c_{ps}(T)/c_{ps}(25)$ decreases linearly with T by slightly less than 2% per degree, at least within the restricted range $25°\mathrm{C} \leq T \leq 35°\mathrm{C}$. This suggests to assume:

$$c^*(T) = \frac{c_{ps}(25)}{c_{ps}(T)}\, c \simeq \frac{c}{1.47 - 0.019T}, \tag{4}$$

[1] Qualitatively, this amounts to state that depletion effects originate from the exclusion from the interparticle gap not of individual micelles, but rather of an entire correlation volume.

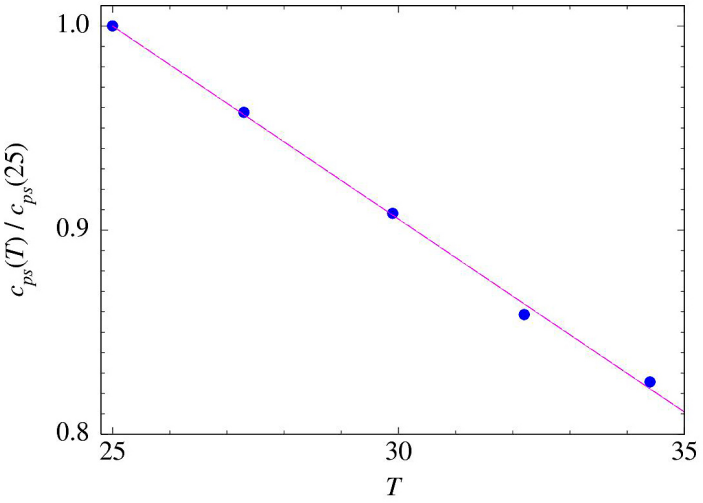

Figure 2: Dependence on temperature T of the depletant concentration $c_{ps}(T)$ where phase separation of a MFA suspension at $\phi = 0.05$, in the presence of 250 mM NaCl, is first observed, scaled to its value $c_{ps}(25)$ at 25°C.

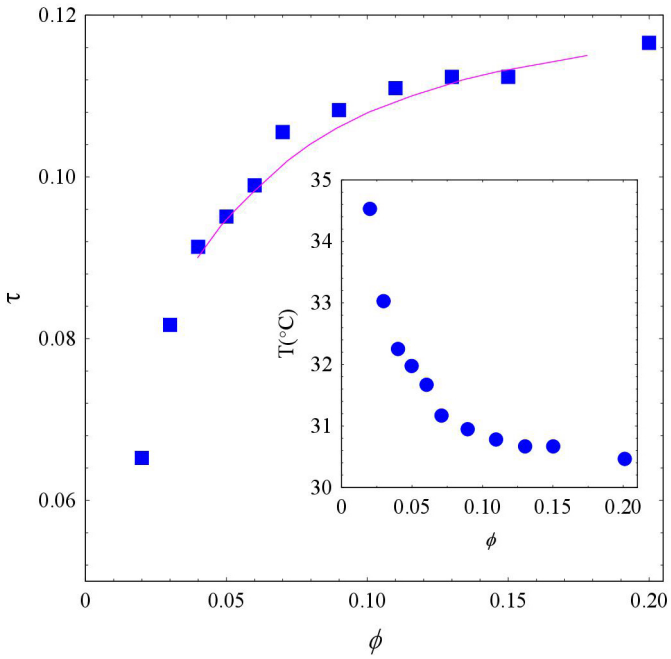

Figure 3: Inset: Volume fraction dependence of the minimal temperature where phase separation is observed at fixed depletant concentration $c = 56\,\mathrm{g/l}$. In the figure body, these data are rescaled using Eq.(4) and (2), and compared to the spinodal line of the AHS model obtained by numerical simulations [5].

where T is in celsius, which allows to define an effective volume fraction $\phi_s^*(T)$ from Eq. (1) to be inserted in Eq. (2) for obtaining the required mapping $\tau(T)$.

It is however important to check whether Eq. 4, which has been obtained for a *fixed* particle volume fraction $\phi = 0.05$, has a more general validity. To this aim, we first measured the phase-separation line $\phi(T)$ at fixed depletant concentration $c = 56$ g/l, chosen for the measurements presented in Fig. 2 of the paper because it allows to closely approach, well within the T-range where the centrifuge can be carefully thermalized ($T < 40°$ C), the metastable L-G coexistence line of the colloid. Using the results of these measurements, which are shown in the inset of Fig. 3, we then mapped $T \to \tau$ with Eq. (2) using the effective concentration given by Eq. (4). The body of Fig. 3 shows that the entire phase separation line $\phi(\tau)$ is in very good agreement with numerical results for the spinodal line of the AHS model [5].

4 Association of β-lactoglobulin

As mentioned in the text, many weak association processes taking place in protein solutions offer an interesting opportunity to investigate the settling of strong attractive particles. For simple colloids interacting via spherically–symmetric attractive potentials, the attraction strength can indeed be increased up to the limit where phase separation occurs. Conversely, the anisotropic, highly stereo–specific protein–protein interactions may just lead to the formation of oligomers, which can be regarded as a kind of micro-phase separation that leave the system macroscopically homogeneous. An interesting example is that of β-lactoglobulin, a milk protein that is present in solution at room temperature as a 36 KDa prolate ellipsoid dimer with semiaxes 1.8 and 3.5 nm [10]. In its natural state, β-lactoglobulin consists of *two* main genetic variants, which can be separated by exploiting a slight difference in their isoelectric points. At lower temperature, and in the narrow pH range ($3.4 <$ pH < 5), one of these variants, BLGA, undergoes a weak but extensive association process. This effect was originally investigated by Timasheff and coworkers in an impressive series of papers, reporting also extensive ultracentrifugation measurements in which both promoted settling and a non-monotonic behavior of $v(\phi)$ were detected [11]. While the former was extensively discussed in terms of chemical reaction models, the ensuing decrease of the sedimentation coefficient for a concentration larger than 15 g/l was simply regarded as "the usual behavior of non-aggregating proteins".

Much later, an extensive light scattering study by Piazza and Iacopini [12] clearly showed that BLGA aggregates, although displaying a well-defined structure (four BLGA dimers associating into an octamer), have an extremely short lifetime, so that they are better physically regarded as "transient clusters". Besides, the non trivial role of "physical" interactions is highlighted by the fact that the aggregation process is first promoted but then fully *frustrated* by increasing the amount of added salt, a rather uncommon effect in colloid science. It is worth noticing that, within the electrolyte concentration range where aggregation is fostered, the reduced virial coefficient can attain values as low as $B_2^* \simeq -2.6$, implying much stronger attractive interactions than those investigated in this work. This arguably accounts for the extensive stretching of the interface observed in recent ultracentrifugation studies of BLGA [14].

For the purpose of this work, it is interesting to point out that a combination of static (SLS) and dynamic (DLS) light scattering data allows to predict the concentration dependence of the settling velocity $v(\phi)$. In fact, the intensity of the light scattered by particles like proteins, which are small compared to the wavelength, is proportional to $\phi S_0(\phi)$, where $S_0(\phi)$ is the structure factor for a suspension at particle volume fraction ϕ in the limit $q = 0$ of zero momentum transfer (which is inversely proportional to the osmotic compressibility of the suspension). On the other hand, the intensity correlation functions measured in DLS experiments allow to extract the collective diffusion coefficient $D_0(\phi)$ in the hydrodynamic limit $q = 0$, which, by the generalized Stokes-Einstein relation,

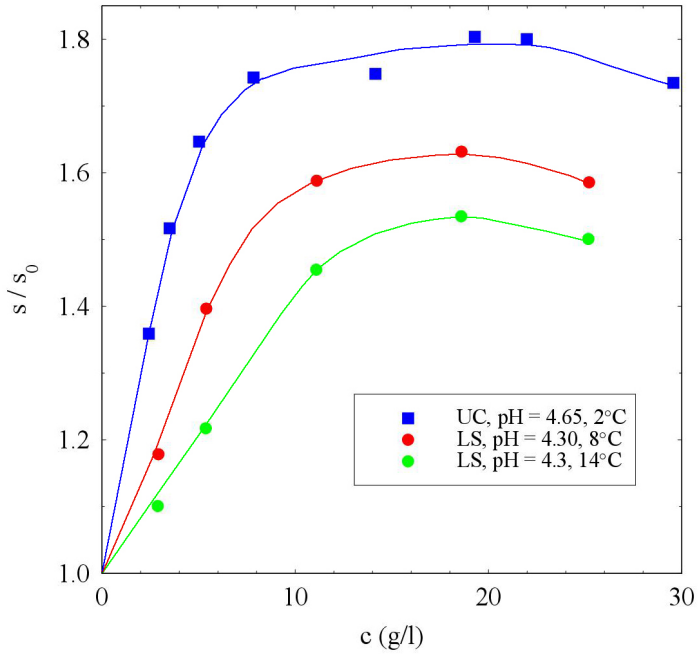

Figure 4: Comparison of the the normalized sedimentation coefficients for BLGA obtained by ultracentrifugation in Ref. [11] to those derived from the light scattering experiment in Ref. [12]. Note that BLGA association gets stronger the lower T, which is arguably the reason why concentration effects are more pronounced for UC than for LS data.

is related to the single-particle Brownian diffusion coefficient D_s by

$$D_0(\phi) = D_s \frac{H_0(\phi)}{S_0(\phi)},$$

where the hydrodynamic factor $H_0(\phi)$, accounting for collective effects on the friction coefficient, can therefore be obtained by a combination of SLS and DLS measurements. However, $H_0(\phi)$ is also the factor which modified the *settling velocity* with respect to the Stokes single-particle value as $v(\phi) = v_s H_0(\phi)$. Notably, the sedimentation velocity can then be evaluated from experiments where nothing actually "settles" (a protein like BLGA requires a centrifugal acceleration a of the order of $10^4 g$ to show any appreciable sedimentation)! The data for $H_0(\phi)$ shown in Fig. 2 of Ref. [12] can therefore be compared to the results for the sedimentation coefficient (the ratio $s(\phi) = v(\phi)/a$) of BLGA displayed in Fig. 7 of Ref. [11]. Fig. 4 shows that the two sets of measurements, although taken at different temperatures and slightly different pH, agree more than qualitatively.

References

[1] D. Frenkel, Physica A, **263**, 26 (1999)

[2] R. P. Sear, J. Chem. Phys. **111**, 2001 (1999)

[3] P. R. ten Wolde and D. Frenkel, Science **277**, 1975 (1997)

[4] R. J. Baxter, J. Chem. Phys. **49**, 2270 (1968).

[5] M. A. Miller and D. Frenkel, J. Chem. Phys. **121**, 535 (2004)

[6] G. Stell, J. Stat. Phys. **63**, 1203 (1991)

[7] S. Buzzaccaro, R. Rusconi, and R. Piazza, Phys. Rev. Lett. **99**, 098301 (2007).

[8] S. Buzzaccaro, R. Piazza, J. Colombo, and A. Parola, J. Chem. Phys. **132**, 124902 (2010).

[9] S. Buzzaccaro, J. Colombo, A. Parola, and R. Piazza, Phys. Rev. Lett. **105**, 198301 (2010).

[10] RCSB Protein Data Bank, structure id: 1beb

[11] R. Townend, R. J. Winterbottom, and S. N. Timasheff, J. Am. Chem. Soc. **82**, 3161 (1960).

[12] R. Piazza and S. Iacopini, Eur. Phys. J. E **7**, 4548 (2002)

[13] R. Piazza, S. Iacopini, and M. Galliano Europhys. Lett. **59**, 149 (2002)

[14] D. Mercadante *et al.*, Biophys. J. **103**, 303 (2012)